Investigating the influence of fine RAP on bituminous mixtures at the mastic scale: viscoelastic analyses and micromechanical modelling

Investigating the influence of fine RAP on bituminous mixtures at the mastic scale: viscoelastic analyses and micromechanical modelling

Seyed Mohsen Motevalizadeh [a], Amir Kavussi [*a], LuciaTsantilis [b], Davide Dalmazzo [b], Ezio Santagata [b]

[a] *Faculty of Civil and Environmental Engineering, Tarbiat Modares University, Tehran, Iran;*

[b] *Department of Environment, Land and Infrastructure Engineering, Politecnico di Torino, Torino, Italy.*

Correspondence details:

Seyed Mohsen Motevalizadeh: mohsen.motevalizadeh@modares.ac.ir;

Amir Kavussi: kavussia@modares.ac.ir;

LuciaTsantilis: lucia.tsantilis@polito.it;

Davide Dalmazzo: davide.dalmazzo@polito.it;

Ezio Santagata: ezio.santagata@polito.it.

Investigating the influence of fine RAP on bituminous mixtures at the mastic scale: viscoelastic analyses and micromechanical modelling

This paper studies the potential effects of RAP fine particles on bituminous mixtures by means of a laboratory investigation performed at the mastic scale. Bituminous mastics, characterized by a constant filler to bitumen volume ratio, were prepared by combining virgin filler and virgin bitumen with several dosages of RAP fine particles. The influence of RAP type was evaluated by employing two RAP products supplied by different sources. The rheological behaviour of the mastics was investigated by means of oscillatory tests carried out with a dynamic shear rheometer. The time-temperature superposition principle and the generalized self-consistent scheme (GSCS) micromechanical model were used to explore the role played by RAP at the mastic scale. Results indicate that the adopted experimental and modelling approach allows a proper assessment of the effects of RAP on the linear viscoelastic properties of mastics and of the degree of blending occurring between virgin and RAP binder.

Keywords: Reclaimed Asphalt Pavement (RAP); bituminous mastic; viscoelasticity; micromechanics; modelling.

Introduction

The use of Reclaimed Asphalt Pavement (RAP) in substitution of virgin aggregates is an absolute priority in the road construction industry. This is due to the savings in environmental and economic costs that derive from the avoided exploitation of natural resources and from the reduction of landfill waste (Arm *et al.* 2017). Past experience has proven that RAP can be successfully employed in all layers of road pavements, including bitumen-bound courses, cement-stabilized foundations, unbound sub-bases and improved subgrades (Santagata *et al.* 2013, Farina *et al.* 2017). However, various technical concerns have originated from research studies focused on the performance properties of bituminous mixtures containing RAP, with the consequent identification of limits to RAP dosage to be adopted in practice. Several researchers have reported that for RAP contents higher than 25 %, a specific and comprehensive mix design is required in order to prevent detrimental effects on pavement

43 performance. In the case of RAP percentages comprised between 15 % and 25 %, a reduction
44 in the grade of virgin binder may be sufficient to account for the stiffening effect induced by
45 RAP, while at percentages lower than 15 % a change in binder grade is not considered to be
46 necessary (McDaniel *et al.* 2002, Copeland 2011).

47 In addition to the effects related to RAP content, one key point that must be
48 thoroughly taken into consideration during the design of bituminous mixtures, is the
49 prediction of the degree of blending that occurs at the interface between virgin binder and
50 aged RAP bitumen (McDaniel *et al.* 2001, Shuai *et al.* 2018). In this regard, three different
51 scenarios can be conjectured to describe the complex system composed of RAP, virgin
52 bitumen and mineral aggregates. These refer to the so-called "black rock", "total blending"
53 and "partial blending" models. According to the "black rock" model, interactions and
54 interdiffusion processes between virgin and aged bitumen are neglected. RAP particles,
55 which are composed of mineral aggregates coated by aged binder, behave as lithic aggregates
56 in the virgin bituminous matrix. In the sector literature it has been reported that this theory
57 can be properly used to model the real behavior of bituminous mixtures only when relatively
58 low RAP contents are used (generally lower than 15 %). On the opposite, in the case of "total
59 blending" it is assumed that the binder from RAP is completely blended with virgin bitumen.
60 In the intermediate scenario of the "partial blending" model, the binder from RAP is
61 considered to be only partially blended with virgin bitumen, with a blending degree that
62 strongly depends upon the specific features of the employed materials and upon mixture
63 production processes (McDaniel *et al.* 2001, 2002, Kriz *et al.* 2014, Rinaldini *et al.* 2014,
64 Shuai *et al.* 2018).

65 The crucial issue of understanding the role played by RAP in bituminous mixtures has
66 been extensively studied in the laboratory at different scales, ranging from the micro-scale
67 (binder level) to the macro-scale (mixture level) (Lee *et al.* 1999, Kriz *et al.* 2014, Rinaldini

68 *et al.* 2014, Mangiafico *et al.* 2019). However, since it is widely recognized that mixture
69 properties are mostly governed by the rheology of the mortar/mastic phase (Craus *et al.* 1978,
70 Underwood and Kim 2011, Hesami *et al.* 2013, Riccardi *et al.* 2018), a significant number of
71 research works have also been carried out at the meso-scale (mortar/mastic level), focusing
72 on the effects due to the presence of RAP in the fine fraction of bituminous mixtures.
73 From the results of an experimental study carried out on bituminous mortars
74 containing RAP and Reclaimed Asphalt Shingle (RAS) materials, Bahia and Swiertz (2011)
75 found that both RAP and RAS strongly affect the linear viscoelastic properties of virgin
76 materials, as proven by stiffness measurements performed at low in-service temperatures.
77 Riccardi et al. (2016) focused on the fatigue properties of mortars containing RAP with the
78 specific purpose of back-calculating the maximum amount of reclaimed material that can be
79 added to Stone Matrix Asphalt (SMA) mixtures. In another research work performed at the
80 mastic scale, Gundla and Underwood (2017) used micromechanical models to predict the
81 degree of blending between RAP binder and newly added bitumen, thereby observing that
82 blending decreases as RAP dosage increases. Mannan et al. (2015) focused their research on
83 the performance properties of RAP mastics at different RAP dosages, demonstrating that
84 RAP mastics exhibit an enhanced rutting resistance. However, it was shown that the use of
85 RAP fines leads to an embrittlement of mastics, with a corresponding increase of their fatigue
86 and low-temperature cracking potential.
87 The research work presented in this paper aims to increase the knowledge about the
88 effects of the presence of RAP in bituminous mixtures, focusing on phenomena occurring at
89 the meso-scale level. Bituminous mastics, characterized by a constant filler to bitumen
90 volume ratio, were prepared in the laboratory by combining virgin filler and virgin bitumen
91 with several dosages of RAP fine particles (composed of filler and aged binder). The effect of
92 RAP type was also evaluated by considering two RAP products supplied by different sources.

The rheological behaviour of the mastics was investigated by means of oscillatory tests carried out with a dynamic shear rheometer. The time-temperature superposition principle and the generalized self-consistent scheme (GSCS) micromechanical model were used to quantify the effects of RAP fine particles on the linear viscoelastic properties of mastics and the degree of blending between virgin and RAP binder, respectively.

MATERIALS AND METHODS

Base materials

The base materials used for the preparation of bituminous mastics included one virgin bitumen, one virgin filler and two types of RAP fine particles.

The virgin bitumen (indicated as BIT), which belonged to the 70/100 penetration grade, was preliminary subjected to rheological and chemical analyses, as detailed in (Santagata *et al.* 2015). These included tests for the evaluation of Performance Grade (PG) and Thin Layer Chromatography (TLC) tests carried out to determine the relative amounts of saturates, aromatics, resins and asphaltenes (SARA analysis). Based on the overall results of the rheological characterization, the bitumen was classified as a PG 58-22 binder. From SARA analysis, the composition of the bitumen was found to correspond to 3.0 % saturates, 65.3 % aromatics, 15.9 % resins, and 15.8 % asphaltenes.

The virgin mineral filler was supplied by an Italian limestone quarry, while the two RAP materials were obtained from an Iranian and an Italian source. RAP fine particles were drawn from the RAP materials by passing them through the 0.075 mm sieve. The resulting fine RAP samples, hereinafter indicated as IR-RAP and IT-RAP, included both uncoated mineral particles and coated clusters of particles containing a combination of aged bitumen and fine aggregates. Due to the lack of additional information, the particle size distribution of virgin filler and RAP filler was assumed to be the same.

Ignition tests were conducted on the two different fine RAPs, as per ASTM D6307, with the twofold objective of retrieving filler particles to be subjected to further characterization tests, and of assessing their bitumen content. This was found to be equal to 11.65 % and 7.84 % (by weight of filler) for IR-RAP and IT-RAP, respectively.

Information regarding the chemical composition of the virgin filler and of the mineral particles recovered from the two types of fine RAP were obtained by making use of X-Ray Fluorescence (XRF) and X-Ray Diffraction (XRD) tests.

From the results presented in Table 1 it can be noticed that the virgin filler was mainly composed of calcium oxide, with a lower non-negligible amount of silica. On the opposite, the Iranian RAP filler (extracted from IR-RAP) was primarily constituted of silica with a lower percentage of calcium oxide, while the Italian RAP filler (coming from IT-RAP) was characterized by intermediate amounts of the two oxides, with a prevalence of silica. All the other components tracked in the test were found in percentages that were always lower than 10 %.

[Table 1 near here]

From the XRD graphs shown in Figure 1 it can be observed that calcite was the predominant element in the virgin mineral filler, while quartz was the main component of both the Iranian and Italian recovered fillers (coming from IR-RAP and IT-RAP, respectively). These results indicate that the virgin mineral filler may be more hydrophobic in comparison to the two fillers retrieved from RAP, with direct implications on interfacial interactions which can be established between mineral particles and the surrounding bitumen in mastics (Pasandín *et al.* 2016). It can be also observed that the outcomes of XRD tests are in good agreement with those obtained from XRF tests (Table 1), with clear correlations existing between SiO_2 and quartz, and between CaO and calcite.

[Figure 1 near here]

142 Specific gravity of the three mineral fillers was determined according to ASTM D854.
143 Filler drawn from the Iranian fine RAP (IR-RAP) exhibited a specific gravity that was similar
144 to that of the reference filler, equal to 2.757 and 2.760, respectively. On the other hand, filler
145 extracted from the Italian fine RAP (IT-RAP) was characterized by a significantly higher
146 value of specific gravity, equal to 2.840.

147 ***Bituminous mastics***

148 Bituminous mastics were prepared in the laboratory by combining fine RAP, virgin filler and
149 virgin bitumen. For all mastics, the filler to bitumen volume ratio was fixed at 27 %, which
150 was considered to be a representative value for typical dense graded bituminous mixtures
151 with 19 mm nominal maximum aggregate size (Gundla and Underwood 2017).
152 Depending upon the case, filler contained in each mastic was composed of a different
153 combination of virgin filler and filler contained in fine RAP. In particular, volumetric
154 concentration of RAP filler (f_{RAP}) was varied between 0 % (for mastics containing
155 exclusively virgin filler) and 100 % (for mastics containing only RAP filler). Additional
156 concentrations considered in the study were set equal to 30 %, 50 %, and 70 %.
157 Mastics were prepared with the five f_{RAP} values indicated above and by making use of
158 the two types of fine RAP (IR-RAP and IT-RAP) referred to in the previous section.
159 Composition of each mastic to be adopted during laboratory preparation was identified by
160 taking into account the results of the preliminary tests carried out to determine RAP binder
161 contents and specific gravity of fillers, and by consequently back-calculating the exact
162 amounts of each component to be employed in order to achieve the target values of filler to
163 bitumen volume ratio (equal to 27 %) and of volumetric concentration of RAP filler (variable
164 between 0 % and 100 %).

Table 2 synthesizes relevant information on the composition of the nine mastics considered in the investigation. Listed parameters include the previously mentioned volumetric concentration of RAP filler (f_{RAP}, expressed with respect to total filler in the mastic), volumetric concentration of RAP binder (b_{RAP}, expressed with respect to total binder in the mastic), volumetric percentages of the four components present in the mastic (virgin bitumen, bitumen from RAP, virgin filler, and filler from RAP), and the filler to bitumen ratio by weight (f/b).

[Table 2 near here]

By analysing the data listed in Table 2 it should be underlined that the mastic with f_{RAP} equal to 0 %, referred to as the virgin mastic (VM), contains exclusively virgin filler and virgin binder and therefore is representative of standard bituminous mixtures. The mastics with f_{RAP} equal to 30 %, 50 % and 70 % (IR-30, IT-30, IR-50, IT-50, IR-70 and IT-70) represent the cases of bituminous mixtures with medium, high and very high RAP dosages, respectively. The mastics with f_{RAP} equal to 100 % (IR-100 and IT-100) are relevant to the case of full replacement of virgin filler in the mastic, although these materials still require the addition of virgin binder to attain the reference 27 % filler to bitumen volume ratio. With respect to the f/b ratios, it can be noticed that values obtained for the mastics prepared with IR-RAP are the same as that calculated for the reference virgin mastic (equal to 1), whereas the mastics containing IT-RAP were characterized by slightly higher values (comprised between 1.01 and 1.03). This is due to the different specific gravity of the filler recovered from IT-RAP with respect to those of both the reference filler and the filler retrieved from IR-RAP.

For the preparation of the bituminous mastics, base materials were mixed by making use of a low-shear mixer at a temperature of 160 °C. Prior to mixing, the virgin filler was heated for 6 hours at 160 °C, while in the case of RAP the conditioning temperature and

duration were set at 110 °C and 2 hours, respectively (McDaniel *et al.* 2001, Gundla and Underwood 2017). After manually blending the virgin filler with RAP in proper proportions, the heated bitumen was added to the compound and mixed with a mechanical stirrer for 60 minutes at a speed of 900 rpm. In order to avoid undesired phase separation between bitumen and filler, blends were poured into metal moulds to obtain beams of 4 mm thickness, and then stored at low temperature.

Testing

The base bitumen and the nine bituminous mastics considered in the investigation were subjected to rheological characterization in the linear viscoelastic domain. Temperature-Frequency Sweep (TFS) tests were carried out by using a dynamic shear rheometer from Anton Paar Inc. (Physica MCR 302), according to AASHTO T 315. Frequency sweeps were performed at several temperatures, comprised between 4 °C and 82 °C, with 6 °C increments between consecutive steps. Thermal conditioning of the specimens was guaranteed by imposing a conditioning time of 12 minutes before each temperature step. Two log-decades of angular frequency were covered during testing, from 1 rad/s to 100 rad/s. The parallel-plate geometry with 8-mm diameter (PP08) and 2-mm gap between plates was used at temperatures comprised between 4 °C and 34 °C, while 25-mm parallel plates (PP25) with 1-mm gap were used between 34 °C and 82 °C. Shear strain values were varied depending upon temperature and frequency conditions, thus allowing the rheological properties of the materials to be always assessed in their linear viscoelastic region. At least two replicates were performed for each test and average results were used in the following analyses.

RESULTS AND DISCUSSION

Raw data analysis

Black and Cole-Cole plots were constructed from raw data of TFS tests in order to perform an overall assessment of the linear viscoelastic properties of the mastics and to verify the applicability of the time-temperature superposition principle. As illustrated in Figure 3a (Black) and 3b (Cole-Cole), these diagrams provide a graphical representation of the norm of the complex modulus $|G^*|$ versus the phase angle δ and of the loss modulus G'' versus the storage modulus G', respectively. By comparing the results obtained for the virgin mastic (VM) with those collected for the mastics prepared with 100 % RAP filler (IR-100 and IT-100), it can be noticed that all materials exhibited continuous single smooth curves. This outcome indicates that all the considered materials showed a rheologically simple response, thus supporting the validity of the time-temperature superposition principle. As expected, it was also observed that the presence of fine RAP affected the rheological behaviour of the mastics to a non-negligible extent.

When considering the results plotted in the Black space, the curve associated to base bitumen (BIT) exhibited the typical gradual transition from a glassy to a viscous state. A similar trend was found for both VM and IT-100, that showed an increase in stiffness and a decrease of the phase angle when approaching the viscous asymptote. In the case of mastics containing IR-RAP, it is worth noting that, besides displaying a higher stiffness at high temperatures (and/or low frequencies), the considered mastic did not show a liquid-like response. This is proven by the phase angle that did not present a monotonic increase at decreasing values of the norm of the complex modulus, thus giving rise to a hump in the Black curves. This behaviour can also be found in TFS tests performed on bituminous mixtures, in which the binder phase is no longer able to lubricate the lithic skeleton particles at high temperatures (Ramirez Cardona *et al.* 2015).

From an inspection of the raw data plotted in the Cole-Cole plane, it can be seen that in the range of low temperatures (and/or high frequencies) the presence of IT-RAP led to an increase in both the storage and the loss moduli. On the other hand, mastics containing IR-RAP showed lower values of the loss modulus, thus indicating that such a fine RAP mainly affected the degree of elasticity exhibited by the material, that shifted towards a more elastic response.

[Figure 2 near here]

For a straightforward comparison of raw data in the same testing conditions, norm and phase angle values of the complex modulus, normalized with respect to those of the virgin mastic, are reported in Table 3 and Table 4, respectively. All results refer to an angular frequency of 10 rad/s and temperatures of 4 °C, 22 °C, 58 °C and 82 °C.

[Table 3 near here]

[Table 4 near here]

As expected, by increasing fine RAP dosage, an increase in $|G^*|$ and a decrease in δ were generally observed. When considering the ratios of the norm of the complex modulus, these values were found to be significantly higher at the higher temperatures. On the contrary, in the case of the phase angle, changes with respect to the reference virgin mastic were more evident at low temperatures and progressively decreased at increasing temperatures, reaching a unit value at the highest investigated temperature (the only exception being IR-100 with a value of 0.98). It is interesting to observe that such trends associated with fine RAP content are coherent with those reported in previous research studies focused on the effects of bitumen ageing (Dalmazzo *et al.* 2019). This seems to suggest that the presence of aged binder coatings around RAP filler particles can have a strong impact on the overall linear viscoelastic response of mastics.

By taking into consideration the effects of the type of fine RAP, it can be clearly noticed that changes were always found to be higher in the case of the IR-RAP, probably as a consequence of the higher volumetric content of aged bitumen and/or a more severe ageing state.

Master curves

By making use of the time-temperature superposition principle, values of the norm and phase angle of the complex modulus were modelled in the form of master curves. Raw data collected from frequency sweep tests carried out at different temperatures were shifted along the frequency axis, thus defining continuous rheological functions at a reference temperature (set equal to 22 °C). Master curves were constructed using an optimization process by means of which experimental data were fitted to the Christensen and Anderson analytical functions (Christensen and Anderson 1992). These are presented in Equations 1 and 2, for the norm and the phase angle of the complex modulus, respectively:

$$|G^*|_{LVE}(\omega_r) = G_g\left[1+\left(\frac{\omega_c}{\omega_r}\right)^{\frac{\text{Log } 2}{R}}\right]^{-\frac{R}{\text{Log } 2}} \quad (1)$$

$$\delta_{LVE}(\omega_r) = \frac{90\ m}{\left[1+\left(\frac{\omega_r}{\omega_c}\right)^{\frac{\text{Log } 2}{R}}\right]} \quad (2)$$

where G_g is the glassy modulus, R is the rheological index, ω_c is the cross over frequency, and ω_r is the reduced angular frequency defined by Equation 3.

$$\omega_R = \omega \cdot a_T \quad (3)$$

where ω is the physical angular frequency and a_T is the shift factor between a generic test temperature T and the reference temperature T_R. Shift factor values at each test temperature were directly derived from the optimization process.

Master curves of the norm and phase angle of the complex modulus are presented in Figure 3 for the base bitumen, the virgin mastic (f_{RAP} equal to 0 %) and the two mastics with

283 f_{RAP} equal to 100 %. For the sake of clarity, results obtained for mastics with intermediate
284 values of f_{RAP} were omitted from the representation since a progressive variation in results
285 was found when increasing the volumetric concentration of RAP filler from 0 % to 100 %.
286 As expected, it can be seen that the presence of the virgin filler caused a general increase in
287 stiffness and elasticity over the entire range of reduced angular frequencies. This is clearly
288 observed when comparing the curves corresponding to VM and BIT. Although to a lesser
289 extent, the incorporation of fine RAP particles also produced an increase in stiffness and
290 elasticity, consistently with the outcomes drawn from raw data analysis presented in the
291 previous section.

292 *[Figure 3 near here]*

293 Curves of the shift factors plotted as a function of temperature are displayed in Figure
294 4, where the results of the mastics containing IR-RAP and IT-RAP (f_{RAP} equal to 100 %) are
295 compared to those of the virgin mastic and of the base bitumen. From an inspection of the
296 plot, it can be seen that at temperatures lower than the reference one, changes were non-
297 negligible only when comparing bitumen and mastics, while a complete overlapping between
298 mastic curves was found. On the contrary, the time-temperature dependency can be
299 discriminated at higher temperatures, where the difference between the generic test
300 temperature and the reference temperature is greater. From a first comparison between base
301 bitumen and virgin mastic, it was highlighted that the presence of filler particles in the
302 bituminous matrix caused a reduction in the high-temperature shift factors. The same trend
303 was observed when analysing the effects of fin RAP in mastics, with a reduction of the
304 high-temperature shift factors at the higher RAP dosage for both mastics containing IR-RAP
305 and IT-RAP.

306 *[Figure 4 near here]*

Thermal susceptibility

In order to gain valuable insights into the effects of fine RAP on the rheological behaviour of mastics, the thermal susceptibility parameter ϑ was evaluated as indicated in Equation 4:

$$\vartheta = \frac{Log[|G^*|(4)/|G^*|(82)]}{Log[a(4)/a(82)]} \quad (4)$$

where $Log[a(4)/a(82)]$ is the difference between the logarithms of the shift factors at 4 °C and 82 °C, , and $Log[|G^*|(4)/|G^*|(82)]$ is the difference between the logarithms of $|G^*|$ at 4 °C and 82 °C (at the reference angular frequency of 10 rad/s).

The main outputs of the analysis are summarised in Figure 5, where the stiffness parameter $Log[|G^*|(4)/|G^*|(82)]$, the time-temperature dependency parameter $Log[a(4)/a(82)]$, and the thermal susceptibility parameter ϑ are presented as a function of both volumetric concentration of RAP filler (f_{RAP}) and volumetric concentration of RAP binder (b_{RAP}). Such a double representation allows the influence of the different phases present in the mastics to be graphically assessed and compared.

$Log[a(4)/a(82)]$ was calculated to analyse the time-temperature dependency, regardless of the value of T_R arbitrarily selected in master curve construction. This parameter, that in the T-$Log\left[a(T)/a\left(T_{ref}\right)\right]$ plot of Figure 4 quantifies the y-axis extension of the curves in the constant range of investigated temperatures (from 4 °C to 82 °C), is a measure of the stretching of master curves in the frequency domain. Hence, higher values of $Log[a(4)/a(82)]$ denote higher extensions of master curves in the axis of reduced angular frequencies.

The evolution of $Log[a(4)/a(82)]$ as a function of f_{RAP} and b_{RAP} are presented in Figure 5a and 5b, respectively. Although a well-defined relationship between time-temperature dependency and mastic volumetrics cannot be clearly identified in both representations, it is evident that an increase in RAP content led to a greater widening of the range of reduced frequencies. Moreover, by comparing $Log[a(4)/a(82)]$ values of neat

bitumen and virgin mastic (both represented in the graph at 0 % RAP content, corresponding to 0 % values of both f_{RAP} and b_{RAP}), the effects induced by the presence of mineral particles in the bituminous matrix can be identified.

Coherently with the above described analysis focused on the stretching of the range of covered frequencies obtained by means of the time-temperature superposition principle, $Log[|G^*|(4)/|G^*|(82)]$ was calculated to quantify the extension of the corresponding range of stiffness values. The parameter $Log[|G^*|(4)/|G^*|(82)]$ is presented as a function of f_{RAP} and b_{RAP} in Figure 5c and 5d, respectively. It is interesting to observe that when plotting the stiffness parameter as a function of the volumetric concentration of RAP filler, two distinct trends can be identified for IR-RAP and IT-RAP. By considering the stiffness parameter as a function of the volumetric concentration of RAP binder, the differences in the two curves are definitely reduced.

[Figure 5 near here]

Plots of ϑ as a function of f_{RAP} (Figure 5e) and b_{RAP} (Figure 5f) reveal information on the effects caused by the presence of fine RAP on the thermal susceptibility of mastics. Although in both representations two distinct curves can be identified, it is worth noting that when plotting thermal susceptibility as a function of the volumetric concentration of RAP binder, a reduction in the divergence between the two curves was obtained, coherently with observations made for the stiffness parameter. These results support the idea that the amount of RAP binder can have a greater impact on the rheology of mastics in comparison to the amount of RAP filler. Focusing on the residual divergence found between IR-RAP and IT-RAP curves in the b_{RAP}- ϑ plot, it can be postulated that part of such a discrepancy can derive from the different RAP filler concentrations associated to constant values of b_{RAP}. Moreover, influencing factors can also include the ageing degree of the two RAP binders and the physicochemical characteristics of the mineral particles composing the different RAP types,

357 that in turn are not the same of those of the virgin mastic. These specific aspects will be
358 certainly explored in future research studies.

359 ***Micromechanical modelling***

360 Further insights into the role played by RAP in bitumen-filler blends were gained by means
361 of micromechanical modelling. When considering the stiffening effect caused by the presence
362 of mineral filler in a bituminous matrix, three main reinforcement contributions can be
363 distinguished: (i) volume-filling reinforcement, related to the presence of rigid inclusions in a
364 softer matrix; (ii) physiochemical reinforcement, generated by interfacial effects between
365 filler and bitumen; and (iii) particle-interaction reinforcement, generated by interconnected
366 contacts between rigid particles which form a networked structure. This last contribution is
367 assumed to be relevant only at relatively high filler concentrations, well above the reference
368 value of 27 % considered in this study.

369 Following the approach developed for traditional bituminous mastics by Buttlar et al.
370 (1999), the stiffening occurring beyond volume filling was quantitatively assessed in all
371 bitumen-filler systems considered in the investigation. The volumetric concentration of
372 spherical inclusions theoretically needed to reach the stiffening level experimentally
373 measured in the laboratory (c_{cal}) was at first calculated by modelling the reinforcement
374 contribution given by volume filling only. Consequently, by subtracting from c_{cal} the real
375 concentration of filler particles (c), the volumetric concentration of hard inclusions not
376 associated to aggregate mineral particles (V_{imm}) was estimated for the virgin mastic and for
377 all mastics containing fine RAP.

378 In Figure 6, a schematic representation of the modelled system composed of spherical
379 inclusions floating in a softer continuous matrix is reported for a virgin mastic (Figure 6a)
380 and for a mastic containing fine RAP (Figure 6b), both characterized by the same volumetric

concentration of mineral filler particles. In neat mastics, V_{imm} can be envisaged as the volumetric concentration of the hard shells of binder around filler particles that are generated by physiochemical phenomena, when the effects of particle-interaction reinforcement are negligible. In the case of mastics containing fine RAP, it is believed that V_{imm} is also significantly affected by the presence of coatings of aged bitumen around RAP filler particles. This is illustrated in Figure 6b, in which a generic system composed of both virgin and RAP filler particles is considered.

[Figure 6 near here]

The stiffening effect generated by volume-filling reinforcement was modelled according to the generalized self-consistent scheme (GSCS) model (Buttlar *et al.* 1999). The corresponding formulation is reported in Equations 5 to 11:

$$A\left(\frac{|G^*|_m}{|G^*|_b}\right)^2 + 2B\left(\frac{|G^*|_m}{|G^*|_b}\right) + C = 0 \quad (5)$$

$$A = 8\left(\frac{G_i}{|G^*|_b} - 1\right)(4 - 5\nu_b)\eta_1 c^{\frac{10}{3}} - 2\left[63\left(\frac{G_i}{|G^*|_b} - 1\right)\eta_2 + 2\eta_1\eta_3\right]c^{\frac{7}{3}} + 252\left(\frac{G_i}{|G^*|_b} - 1\right)\eta_2 c^{\frac{5}{3}} - 50\left(\frac{G_i}{|G^*|_b} - 1\right)(7 - 12\nu_b + 8\nu_b^2)\eta_2 c + 4(7 - 10\nu_b)\eta_2\eta_3 \quad (6)$$

$$B = -4\left(\frac{G_i}{|G^*|_b} - 1\right)(1 - 5\nu_b)\eta_1 c^{\frac{10}{3}} + 4\left[63\left(\frac{G_i}{|G^*|_b} - 1\right)\eta_2 + 2\eta_1\eta_3\right]c^{\frac{7}{3}} - 504\left[\left(\frac{G_i}{|G^*|_b} - 1\right)\eta_2\right]c^{\frac{5}{3}} + 150\left(\frac{G_i}{|G^*|_b} - 1\right)(3 - \nu_b)\nu_b\eta_2 c + 3(15\nu_b - 7)\eta_2\eta_3 \quad (7)$$

$$C = 4\left(\frac{G_i}{|G^*|_b} - 1\right)(5\nu_b - 7)\eta_1 c^{\frac{10}{3}} - 2\left[63\left(\frac{G_i}{|G^*|_b} - 1\right)\eta_2 + 2\eta_1\eta_3\right]c^{\frac{7}{3}} + 252\left(\frac{G_i}{|G^*|_b} - 1\right)\eta_2 c^{\frac{5}{3}} + 25\left(\frac{G_i}{|G^*|_b} - 1\right)(\nu_b^2 - 7)\eta_2 c - (7 + 5\nu_b)\eta_2\eta_3 \quad (8)$$

$$\eta_1 = \left(\frac{G_i}{|G^*|_b} - 1\right)(49 - 50\nu_i\nu_b) + 35\frac{G_i}{|G^*|_b}(\nu_i - 2\nu_b) + 35\,(2\nu_i - \nu_b) \quad (9)$$

$$\eta_2 = 5\nu_i\left(\frac{G_i}{|G^*|_b} - 8\right) + 7\left(\frac{G_i}{|G^*|_b} + 4\right) \quad (10)$$

$$\eta_3 = \frac{G_i}{|G^*|_b}(8 - 10\nu_b) + (7 - 5\nu_b) \quad (11)$$

where $|G^*|_m$ and $|G^*|_b$ are the norm of the complex modulus of mastic and bitumen (collected from direct measurements); G_i is the shear modulus of inclusions (set equal to 24 GPa); ν_b and ν_i are the Poisson ratios of bitumen and inclusions (set equal to 0.40 and 0.15, respectively).

By back-calculating the values of c that lead to a convergence between predicted and measured $|G^*|_m$ data by means of Equations 5 to 11, the effective volumetric concentration of filler (c_{cal}) was computed. With the purpose of taking into account the role of temperature in stiffening effects, the optimization process was performed separately at each test temperature by considering only $|G^*|$ values collected at the reference angular frequency of 10 rad/s. V_{imm} was then calculated as the difference between the effective volume concentration, which takes into consideration the spherical inclusions composed of both filler particles and influenced binder layers, and the actual filler concentration (Equation 12).

$$V_{imm} = c_{cal} - c \quad (12)$$

The outcomes of micromechanical modelling are summarized in Figure 7a, where V_{imm} is plotted as a function of the volumetric concentration of RAP binder (b_{RAP}). For the sake of clarity, only results obtained at 4 °C, 10 °C, 22 °C and 58 °C are displayed in the graph.

[Figure 7 near here]

For values of b_{RAP} equal to 0 % (which correspond to the case of the virgin mastic), it can be seen that the stiffening effect associated with interfacial phenomena taking place between filler and bitumen was of the same order of magnitude of the actual filling contribution. This was proven by the V_{imm} values, comprised between 0.14 and 0.20, that are comparable to the volumetric concentration of filler, equal to 0.27. Moreover, it is interesting to observe that the value of V_{imm} depends on test temperature, showing higher values at increasing temperatures.

Regardless of the considered temperature, mastics containing fine RAP showed superior values of the "fictitious" immobilized binder, coherently with the outcomes of the overall rheological characterization. By analysing the relation between V_{imm} and b_{RAP}, linear trends were highlighted at each test temperature regardless of RAP origin, with V_{imm} values

431 approaching those found for the virgin mastic at b_{RAP} values tending to zero. From a general
432 overview of the results, it can be stated that the layer of binder immobilized by virgin filler is
433 significantly smaller than the layer activated by RAP mineral particles. While in the case of
434 virgin mastics it is believed that the dimension of spherical inclusions is mainly governed by
435 bitumen-filler interfacial phenomena, in the case of mastics containing fine RAP, these
436 effects are also mixed with interactions triggered by the aged binder coatings of RAP filler
437 particles. Moreover, it can be hypothesised that the increased dimensions of the RAP
438 spherical inclusions can also promote the onset of local particle-to-particle interaction
439 reinforcement effects.

440 When focusing on the influence of temperature on V_{imm}, it can be noticed that in line
441 with the trend highlighted for the virgin mastic (displayed in the plot at b_{RAP} equal to 0 %), at
442 increasing temperatures the sensitivity of V_{imm} on the amount of RAP binder dramatically
443 increased. This is proven by the V_{imm} values that, at the maximum value of b_{RAP}, were
444 doubled passing from 4 °C to 58 °C. Such a finding can be partially explained by considering
445 the difference in stiffness between the neat bituminous matrix and the immobilized binder
446 constituting the rigid shells which cover filler particles. At low temperatures this difference is
447 expected to be limited since all bituminous materials asymptotically tend to a glassy modulus.
448 On the other hand, at high temperatures the altered bitumen, generated by interfacial
449 phenomena and/or ageing, seemed to be less sensitive to temperature variations with respect
450 to the bitumen composing the matrix phase. This result is also consistent with the reduction in
451 thermal susceptibility found at increasing b_{RAP} values (Figure 5f). Based on these
452 observations, it can be concluded that at low temperatures the effects produced by fine RAP
453 can be adequately described by the “total blending” model, as revealed by the slight
454 differences in V_{imm} values found between virgin mastic and blends containing RAP. On the

455 opposite, by increasing temperature, the response of the mastics containing RAP definitely
456 deviates from that predicted with a “total blending” approach.
457 In order to further discriminate between the stiffening provided by the RAP aged
458 binder and other reinforcement effects, the “black rock” hypothesis was also considered.
459 While according to the “total blending” approach the binder deriving from RAP is treated in
460 modelling as the binder constituting the matrix phase, in the “black rock” approach the
461 volume of RAP binder is considered as part of the filler volume concentration. The
462 corresponding definition of immobilized binder in the “black rock” hypothesis is given in
463 Equation 13:
464 $V_{imm} = c_{cal} - (c + b_{RAP})$ (13)
465 As shown in Figure 7b, by totally excluding RAP binder from the volume of
466 immobilized binder, further effects related to physiochemical phenomena and other
467 contributions deriving from contact reinforcement can be highlighted. At high temperatures,
468 V_{imm} still increased for increasing b_{RAP} values, thus indicating that in mastics containing
469 RAP, stiffening effects are not exclusively related to the presence of the hard aged bitumen
470 coming from RAP. While at intermediate temperatures V_{imm} was almost constant, at low
471 temperatures a decrease in V_{imm} was observed. This last result suggests that the presence of
472 the aged RAP binder can hinder interfacial effects occurring between the bitumen of the
473 matrix phase and filler particles, thus confirming a deviation from the “black rock”
474 hypothesis at low temperatures.
475 In the assumption that mastics containing RAP will exhibit intermediate behaviours
476 between those depicted in the extreme ideal cases of “total blending” and “black rock”,
477 results displayed in Figure 7a and Figure 7b represent the range of immobilized binder
478 volumes that can actually form in any mastic as a function of RAP dosage.

Conclusions

Based on the results presented in this paper, it can be concluded that fine RAP can have a significant impact on the overall rheological behaviour of mastics. This outcome strongly suggests that the use of fine RAP in substitution of virgin filler requires a thorough characterization of base materials in order to avoid detrimental effects on pavement performance. In such a context, the micromechanical approach adopted in the present study has proven to be an effective tool to assess the role played by RAP at the mastic scale.

Mastics containing RAP always showed higher stiffness and elasticity, which progressively increased at increasing RAP dosages to an extent that was dependent on RAP type. It was observed that RAP caused an overall reduction in the thermal susceptibility of mastics, that was mainly related to the volumetric concentration of RAP binder. However, it is worth noting that the type of RAP also affected the thermal dependency of mastics, probably as a consequence of the key role played by the ageing degree of different RAP binders and/or by the physicochemical characteristics of RAP mineral particles.

From the micromechanical modelling it was highlighted that RAP particles generate higher volume concentrations of fictitious immobilized bitumen, used to quantitatively assess the stiffening effects in mastics beyond volume filling. While the influence of RAP source was quite limited, the volume of bitumen behaving as a hard coating around mineral inclusions was found to be strongly dependent upon temperature, thus indicating the need to perform an extensive viscoelastic characterization of the composite materials.

Further studies are needed in order to support the findings of this research work, possible by extending the investigation to the macro-scale with an appropriate characterization of the viscoelastic and damage properties of bituminous mixtures containing different types and quantities of fine RAP. Modelling can also be improved by adopting a multi-scale approach,

503 with the final goal of fully understanding the implications of RAP use in bituminous
504 mixtures.

505 **References**

506 Arm, M., Wik, O., Engelsen, C.J., Erlandsson, M., Hjelmar, O., and Wahlström, M., 2017.
507 How Does the European Recovery Target for Construction & Demolition Waste Affect
508 Resource Management? *Waste and Biomass Valorization*, 8 (5), 1491–1504.

509 Bahia, H.U. and Swiertz, D., 2011. Design System for HMA Containing a High Percentage
510 of RAS Material (RMRC Project 66).

511 Buttlar, W.G., Bozkurt, D., Al-Khateeb, G.G., and Waldhoff, A.S., 1999. Understanding
512 asphalt mastic behavior through micromechanics. *Transportation Research Record*,
513 (1681), 157–169.

514 Christensen, D.W. and Anderson, D.A., 1992. Interpretation of dynamic mechanical test data
515 for paving grade asphalt. *Journal of the Association of Asphalt Paving Technologists*,
516 61, 67–116.

517 Copeland, A., 2011. Reclaimed Asphalt Pavement in Asphalt Mixtures: State of the Practice.
518 *Report No. FHWA-HRT-11-021*, (FHWA), McLean, Virginia.

519 Craus, J., Ishai, I., and Sides, A., 1978. Some Physico-Chemical Aspects of the Effect and the
520 Role of the Filler in Bituminous Paving Mixtures. *Journal of the association of Asphalt*
521 *Paving Technologists*, 47, 558–588.

522 Dalmazzo, D., Jiménez Del Barco Carrión, A., Tsantilis, L., Lo Presti, D., and Santagata, E.,
523 2019. Non- petroleum- based binders for paving applications: Rheological and chemical
524 investigation on ageing effects. *In*: *Proceedings of the 5th International Symposium on*
525 *Asphalt Pavements & Environment*. Padova, Italy, 67–76.

526 Farina, A., Zanetti, M.C., Santagata, E., and Blengini, G.A., 2017. Life cycle assessment
527 applied to bituminous mixtures containing recycled materials: Crumb rubber and
528 reclaimed asphalt pavement. *Resources, Conservation and Recycling*, 117, 204–212.

529 Gundla, A. and Underwood, S., 2017. Evaluation of in situ RAP binder interaction in asphalt
530 mastics using micromechanical models. *International Journal of Pavement Engineering*,
531 18 (9), 798–810.

Hesami, E., Ghafar, A.N., Birgisson, B., and Kringos, N., 2013. Multi-scale Characterization of Asphalt Mastic Rheology. *In*: *Kringos N., Birgisson B., Frost D., Wang L. (eds) Multi-Scale Modeling and Characterization of Infrastructure Materials*. RILEM Bookseries, vol. 8. Springer, Dordrecht, 45–61.

Kriz, P., Grant, D.L., Veloza, B.A., Gale, M.J., Blahey, A.G., Brownie, J.H., Shirts, R.D., and Maccarrone, S., 2014. Blending and diffusion of reclaimed asphalt pavement and virgin asphalt binders. *Road Materials and Pavement Design*, 15 (1), 78–112.

Lee, K.W., Soupharath, N., Shukla, A., Franco, C.A., and Manning, F.J., 1999. Rheological and mechanical properties of blended asphalts containing recycled asphalt pavement binders. *Journal of the Association of Asphalt Paving Technologists*, 68, 89–128.

Mangiafico, S., Sauzéat, C., and Di Benedetto, H., 2019. Comparison of different blending combinations of virgin and RAP-extracted binder: Rheological simulations and statistical analysis. *Construction and Building Materials*, 197, 454–463.

Mannan, U.A., Islam, M., Weldegiorgis, M., and Tarefder, R., 2015. Experimental investigation on rheological properties of recycled asphalt pavement mastics. *Applied Rheology*, 25 (2).

McDaniel, R.S., Soleymani, H., Anderson, R.M., Turner, P., and Peterson, R., 2001. *Recommended Use of Reclaimed Asphalt Pavement in the Superpave Mix Design Method*. NCHRP Rep. 452. Washington, DC.

McDaniel, R.S., Soleymani, H., and Shah, A., 2002. Use of Reclaimed Asphalt Pavement (RAP) Under Superpave Specifications : A Regional Pooled Fund Project. Publication FHWA/IN/JTRP-2002/06. *Fhwa*, (May), p.

Pasandín, A.R., Pérez, I., Ramírez, A., and Cano, M.M., 2016. Moisture damage resistance of hot-mix asphalt made with paper industry wastes as filler. *Journal of Cleaner Production*, 112, 853–862.

Ramirez Cardona, D.A., Pouget, S., Di Benedetto, H., and Olard, F., 2015. Viscoelastic behaviour characterization of a gap-graded asphalt mixture with SBS polymer modified bitumen. *Materials Research*, 18 (2), 373–381.

Riccardi, C., Cannone Falchetto, A., Losa, M., and Wistuba, M., 2016. Back-calculation method for determining the maximum RAP content in Stone Matrix Asphalt mixtures with good fatigue performance based on asphalt mortar tests. *Construction and Building*

563 *Materials*, 118, 364–372.

564 Riccardi, C., Cannone Falchetto, A., Losa, M., and Wistuba, M.P., 2018. Development of
565 simple relationship between asphalt binder and mastic based on rheological tests. *Road*
566 *Materials and Pavement Design*, 19 (1), 18–35.

567 Rinaldini, E., Schuetz, P., Partl, M.N., Tebaldi, G., and Poulikakos, L.D., 2014. Investigating
568 the blending of reclaimed asphalt with virgin materials using rheology, electron
569 microscopy and computer tomography. *Composites Part B: Engineering*, 67, 579–587.

570 Santagata, E., Baglieri, O., Tsantilis, L., and Chiappinelli, G., 2015. Fatigue and healing
571 properties of nano-reinforced bituminous binders. *International Journal of Fatigue*, 80,
572 30–39.

573 Santagata, E., Blengini, G.A., Farina, A., Zanetti, M.C., and Engineering, I., 2013. Life Cycle
574 Assessment of Road Pavement Base and Foundation Courses Containing Reclaimed
575 Asphalt Pavement (RAP). *In*: *Proceedings Sardinia, Fourteenth International Waste*
576 *Management and Landfill Symposium*. S. Margherita di Pula, Italy.

577 Shuai, Y., Shen, S., Zhou, X., and Li, X., 2018. Effect of partial blending on high content
578 reclaimed asphalt pavement (RAP) mix design and mixture properties. *Transportation*
579 *Research Record: Journal of the Transportation Research Board*, 2672 (28), 79–87.

580 Underwood, B.S. and Kim, Y.R., 2011. Experimental investigation into the multiscale
581 behaviour of asphalt concrete. *International Journal of Pavement Engineering*, 12 (4),
582 357–370.

583 Table 1. Results of XRF tests carried out on fillers.

Components	**Percentages**		
	Virgin mineral filler	Iranian RAP filler	Italian RAP filler
SiO2	10.651	51.518	35.073
CaO	44.644	15.855	27.095
Al2O3	1.304	7.359	4.849
Na2O	0.048	2.016	0.928
MgO	3.712	3.253	5.087
K2O	0.471	2.888	1.169
Fe2O3	1.006	4.784	4.051
Other components	0.324	2.127	1.848

584

585 Table 2. Composition of mastics.

Fine RAP type	Mastic ID	Volumetric concentration of RAP filler, (f_{RAP})	Volumetric concentration of RAP binder, (b_{RAP})	Volumetric percentages in bituminous mastic				Filler to bitumen ratio by weight, (f/b)
				Virgin binder	Binder from RAP	Virgin Filler	Filler from RAP	
-	VM	0	0.0	73.0	0.0	27.0	0.0	1.00
IR- RAP	IR-30	30	4.0	70.1	2.9	18.9	8.1	1.00
	IR-50	50	6.6	68.2	4.8	13.5	13.5	1.00
	IR-70	70	9.2	66.3	6.7	8.1	18.9	1.00
	IR-100	100	13.2	63.4	9.6	0.0	27.0	1.00
IT- RAP	IT-30	30	2.6	71.1	1.9	18.9	8.1	1.01
	IT-50	50	4.4	69.8	3.2	13.5	13.5	1.02
	IT-70	70	6.1	68.5	4.5	8.1	18.9	1.02
	IT-100	100	8.8	66.6	6.4	0.0	27.0	1.03

586

587 Table 3. |G*| ratios for mastics containing IR-RAP (variable volumetric concentration of
588 RAP filler).

$\|G^*\|$ ratios	IR-30	IR-50	IR-70	IR-100	IT-30	IT-50	IT-70	IT-100
4	1.04	1.11	1.17	1.12	1.13	1.14	1.15	1.30
22	1.25	1.40	1.60	1.70	1.22	1.27	1.35	1.58
58	1.34	1.48	1.86	2.17	1.15	1.27	1.52	1.74
82	1.19	1.31	1.61	1.80	1.15	1.25	1.44	1.63

589

590 Table 4. δ ratios for mastics containing IR-RAP (variable volumetric concentration of RAP
591 filler).

δ ratios	IR-30	IR-50	IR-70	IR-100	IT-30	IT-50	IT-70	IT-100
4	0.92	0.89	0.88	0.84	0.95	0.94	0.93	0.91
22	0.96	0.94	0.93	0.90	0.97	0.96	0.95	0.94
58	0.99	0.99	0.99	0.98	1.00	1.00	0.99	0.99
82	1.00	1.00	1.00	0.98	1.00	1.01	1.01	1.00

592

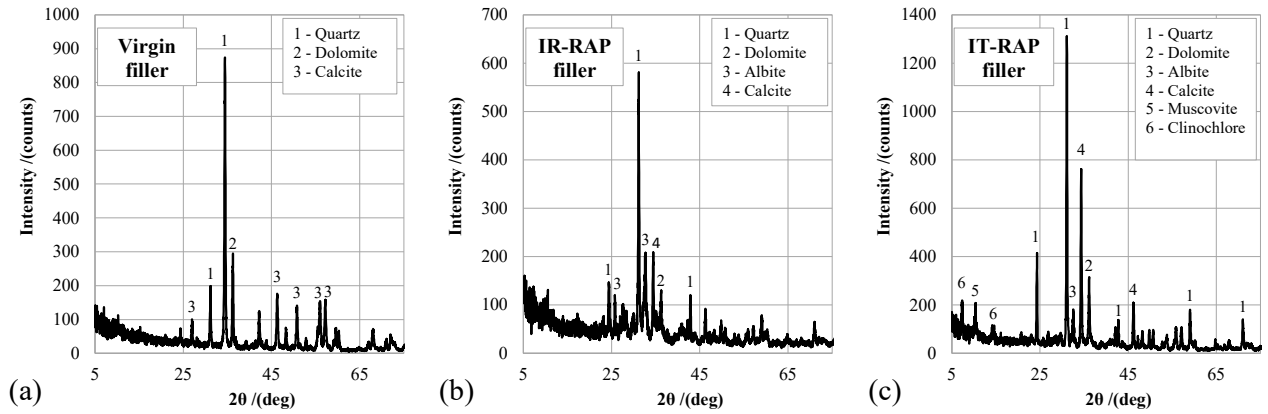
Virgin filler
1 - Quartz
2 - Dolomite
3 - Calcite
Intensity /(counts)
2θ /(deg)
(a)
IR-RAP filler
1 - Quartz
2 - Dolomite
3 - Albite
4 - Calcite
Intensity /(counts)
2θ /(deg)
(b)
IT-RAP filler
1 - Quartz
2 - Dolomite
3 - Albite
4 - Calcite
5 - Muscovite
6 - Clinochlore
Intensity /(counts)
2θ /(deg)
(c)

[Figure 1]

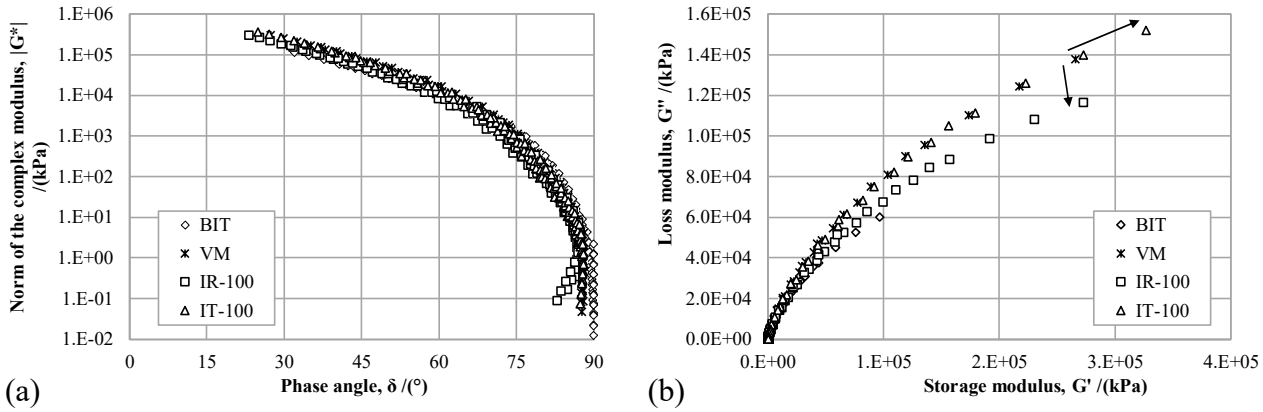

595

596 [Figure 2]

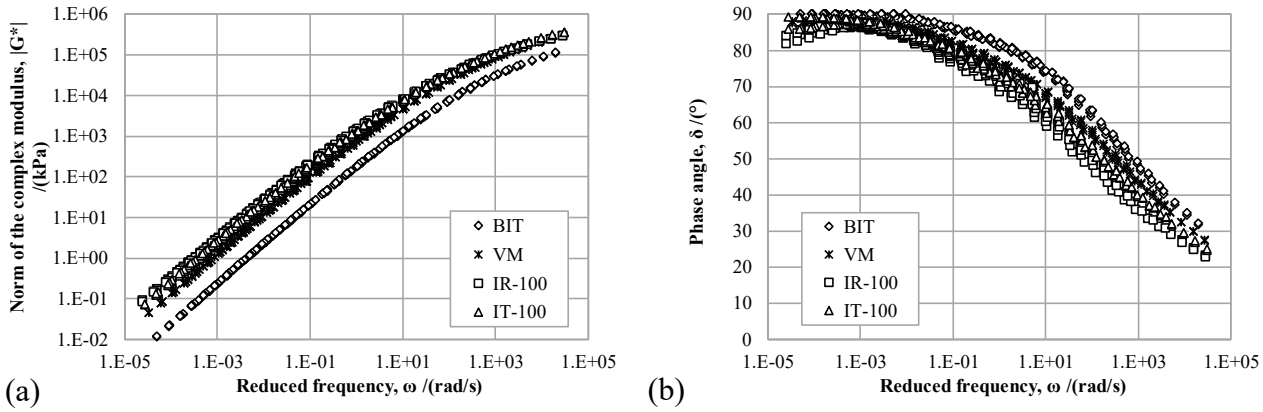
Norm of the complex modulus, |G*| /(kPa)
1.E+06
1.E+05
1.E+04
1.E+03
1.E+02
1.E+01
1.E+00
1.E-01
1.E-02
1.E-05
1.E-03
1.E-01
1.E+01
1.E+03
1.E+05
Reduced frequency, ω /(rad/s)
BIT
VM
IR-100
IT-100
(a)
Phase angle, δ /(°)
90
80
70
60
50
40
30
20
10
0
Reduced frequency, ω /(rad/s)
BIT
VM
IR-100
IT-100
(b)

[Figure 3]

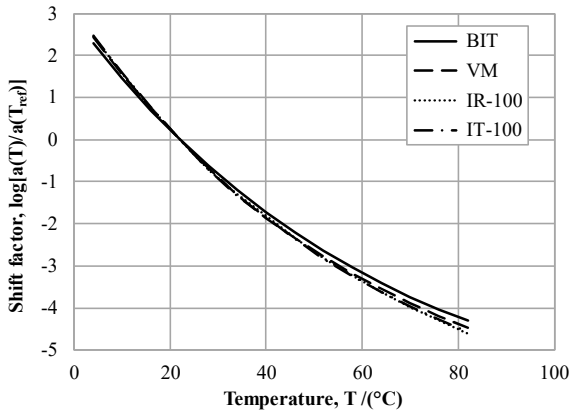

599

600 [Figure 4]

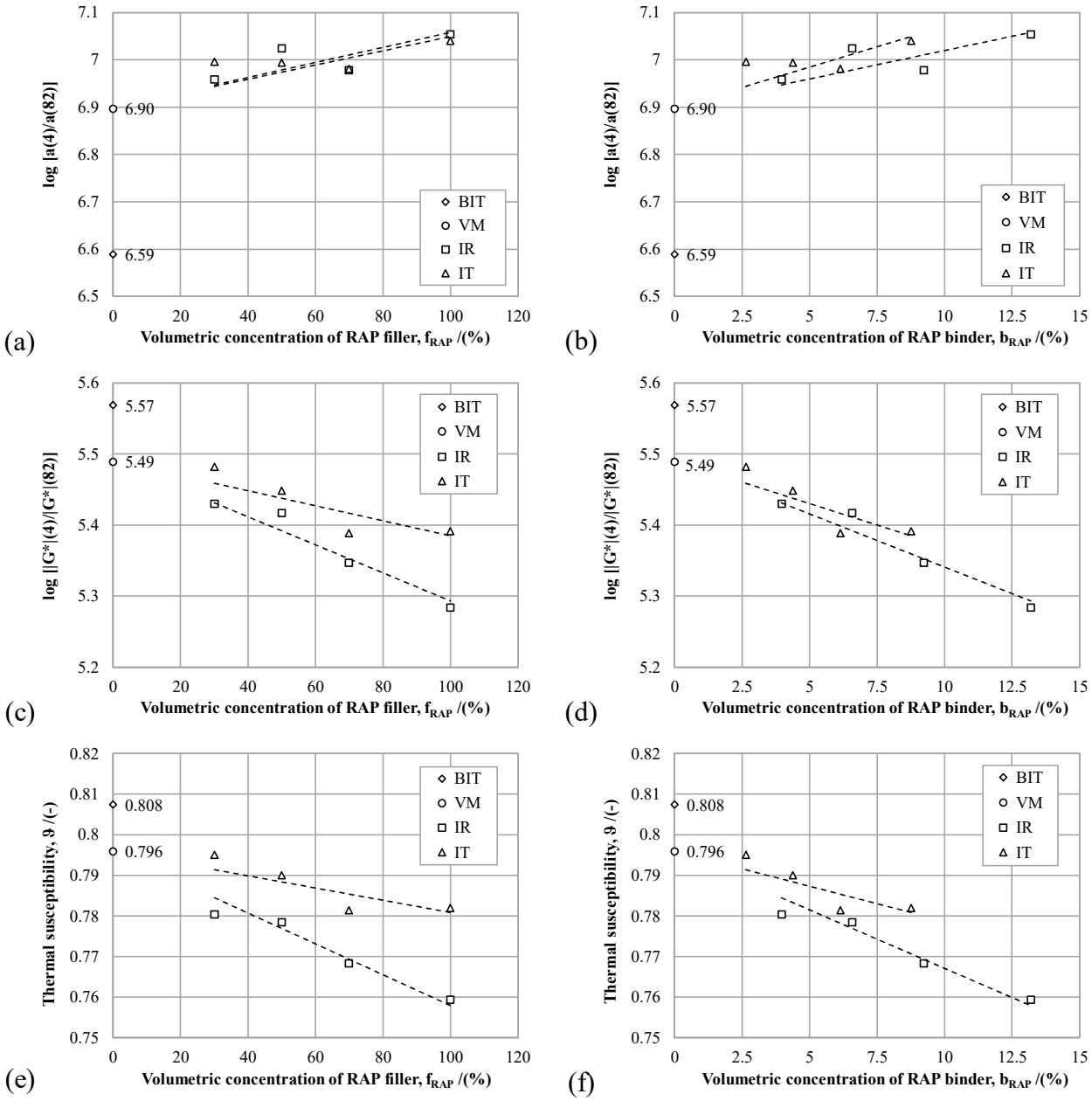
(a)
log [a(4)/a(82)]
6.90
6.59
BIT
VM
IR
IT
Volumetric concentration of RAP filler, f_{RAP} /(%)
(b)
log [a(4)/a(82)]
6.90
6.59
BIT
VM
IR
IT
Volumetric concentration of RAP binder, b_{RAP} /(%)
(c)
log ||G*|(4)/|G*|(82)]
5.57
5.49
BIT
VM
IR
IT
Volumetric concentration of RAP filler, f_{RAP} /(%)
(d)
log ||G*|(4)/|G*|(82)]
5.57
5.49
BIT
VM
IR
IT
Volumetric concentration of RAP binder, b_{RAP} /(%)
(e)
Thermal susceptibility, ϑ /(-)
0.808
0.796
BIT
VM
IR
IT
Volumetric concentration of RAP filler, f_{RAP} /(%)
(f)
Thermal susceptibility, ϑ /(-)
0.808
0.796
BIT
VM
IR
IT
Volumetric concentration of RAP binder, b_{RAP} /(%)

[Figure 5]

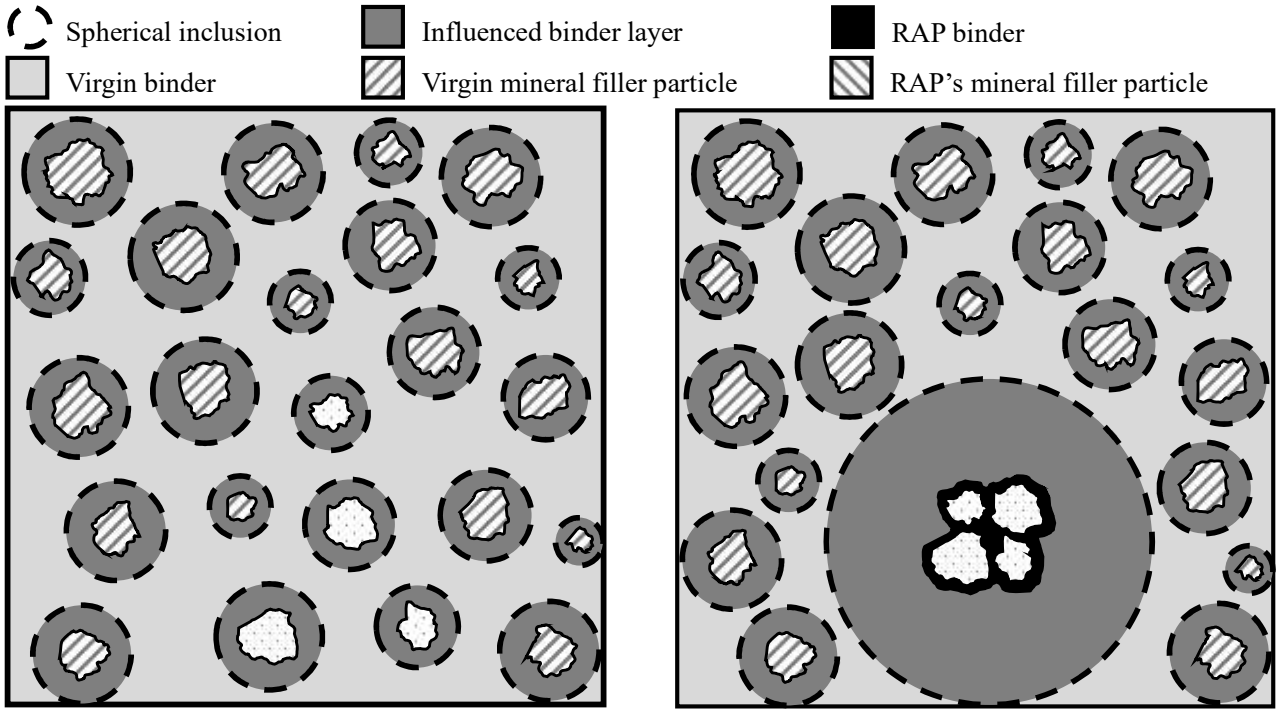

(a) Mineral filler + virgin bitumen

(b) Mineral filler + RAP + virgin bitumen

603

604 [Figure 6]

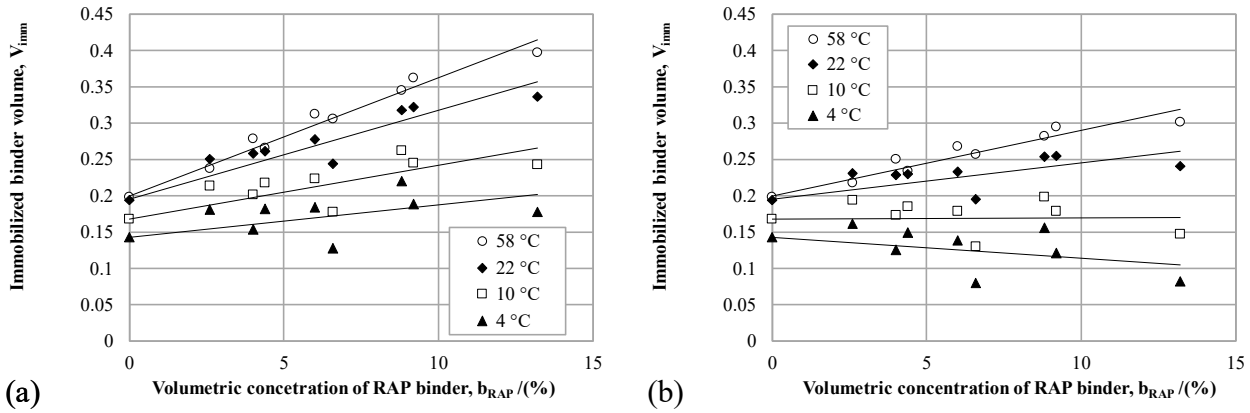
Immobilized binder volume, V_{imm}
0.45
0.4
0.35
0.3
0.25
0.2
0.15
0.1
0.05
0
0
5
10
15
58 °C
22 °C
10 °C
4 °C
Volumetric concetration of RAP binder, b_{RAP} /(%)
(a)
Immobilized binder volume, V_{imm}
58 °C
22 °C
10 °C
4 °C
Volumetric concentration of RAP binder, b_{RAP} /(%)
(b)

[Figure 7]

Figure Captions:

Figure 1. Results of XRD tests carried out on fillers: (a) virgin filler, (b) IR-RAP filler and (c) IT-RAP filler.

Figure 2. (a) Black and (b) Cole-Cole diagrams of mastics.

Figure 3. Master curves of the norm (a) and the phase angle (b) of the complex modulus.

Figure 4. Shift factors of mastics ($T_{ref.}$ = 22 °C).

Figure 5. (a, b) $Log[a(4)/a(82)]$, (c, d) $Log(|G^*|_4/|G^*|_{82})$, and (e, f) ϑ as a function of RAP volumetric concentration of RAP filler and RAP binder.

Figure 6. Representation of particulate composite structure for generic mastic (a) and mastic containing RAP particles (b).

Figure 7. V_{imm} as a function of volumetric concentration of RAP binder according to (a) "total blending" and (b) "black rock" hypotheses.